Astron. Astrophys. 351, 472–476 (1999)

ASTRONOMY AND ASTROPHYSICS

OH lines in the FIR spectra of the OH megamaser galaxies IRAS 20100-4156 and 3Zw35*

W.H. Kegel[1], **T. Hertenstein**[1], **and A. Quirrenbach**[2]

[1] Institut für Theoretische Physik der Universität Frankfurt am Main, Postfach 111932, 60054 Frankfurt am Main, Germany
[2] University of California, San Diego, Department of Physics, Center of Astrophysics and Space Sciences, 9500 Gilman Drive, La Jolla, CA 92093-0424, USA

Received 12 April 1999 / Accepted 16 August 1999

Abstract. Using the SWS and LWS instruments on board of the ISO spacecraft, we searched for OH-lines in the FIR spectra of the two OH megamaser galaxies IRAS 20100-4156 and 3 Zw 35. The lines at 34 μ and 53 μ were detected in absorption with certainty in the spectrum of IRAS 20100-4156 and probably in the spectrum of 3 Zw 35. From the measured equivalent widths we derived column densitites of $N_{OH} \approx (2.2 \pm 0.4)$ $\cdot 10^{17}$ cm^{-2} and $N_{OH} \approx (2.0 \pm 0.6) \cdot 10^{17}$ cm^{-2}, respectively. The 119 μ line was tentatively detected in the spectrum of IRAS 20100-4156, but definitely is much weaker than would be expected from the strengths of the lines at 34 μ and 53 μ. In the spectrum of 3 Zw 35 the 119 μ line was not found. We take this as an indication that at 119 μ the continuum source is considerably larger than at 34 μ and 53 μ and is covered only partly by the absorbing OH cloud. - The finding that the OH column density is similar in both objects despite substantial differences in their IR and maser luminosities, is taken as support of the hypothesis that OH megamasers are radiatively pumped by the $34\,\mu$ and/or the $53\,\mu$ lines.

Key words: galaxies: active – galaxies: individual: IRAS 20100-4156 – galaxies: individual: 3Zw35 – masers – ISM: molecules – infrared: galaxies

1. Introduction

In order to study the pump mechanism in OH megamaser galaxies we performed extensive radiative transfer calculations in an on-the-spot approximation. Our model accounts for radiative pumping by FIR radiation and for the effects of line overlap caused by a molecular outflow (or infall). One of the results is that under conditions leading to population inversion for the 1667 MHz line, we also find weak inversion for the $\left(^2\Pi_{1/2}, \mathrm{J}=5/2 \rightarrow {}^2\Pi_{3/2}, \mathrm{J}=7/2\right)$ transition. Motivated by this tentative prediction of an iraser line at 115 μ, we searched for OH lines in the FIR spectra of two OH megamaser galaxies. The spectra were taken with the ISO Short-Wavelength and Long-Wavelength spectrometer, respectively. We searched for the putative iraser line at 115 μ as well as for the lines at 34 μ, 53 μ, and 119 μ. The latter three lines all connect to the rotational ground state and are predicted by our computations to occur in absorption.

As targets we chose IRAS 20100-4156 and 3 Zw 35. IRAS 20100-4156 is the second most luminous and the second most distant $(z = 0.129)$ OH megamaser galaxy known. The (isotropic) luminosity emitted in the 1667 MHz line is of the order of $10^4 L_\odot$ (Staveley-Smith et al. 1989).It belongs to the class of ultraluminous galaxies, having an IR luminosity of about $2 \cdot 10^{12} L_\odot$. According to Duc et al. 1997 it appears to be a system of two disk galaxies in collision. The R-band image shows clearly two nuclei separated by $2\overset{''}{.}7$ or 5.4 kpc.

3 Zw 35 is a more or less average OH megamaser galaxy at a redshift of $z = 0.0276$. The (isotropic) luminosity of its OH maser emission is about 540 $L_\odot$ and its IR luminosity is $3 \cdot 10^{11} L_\odot$ (Chapman et al. 1990). Similar to IRAS 20100-4156, 3 Zw 35 is a double system. The OH maser emission is associated with the brighter northern component which has been classified by Chapman et al. 1990 either as a LINER or a Seyfert 2 galaxy.

2. Observations and data reduction

For both objects we observed small spectral ranges covering the positions of the OH lines at 34 μ, 53 μ, 115 μ, and 119 μ (rest frame wavelengths). With the LWS we took on-source and off-source spectra. The observational parameters are given in Table 1. The spectrum of IRAS 20100-4156 observed on Nov. 9th, 1996 seemed to show some emission roughly at the position of the 115 μ line, but the observational data were not conclusive. We therefore took in March 1998 an additional spectrum covering only the region of the 115 μ line. - For 3 Zw 35 we took in addition a low resolution spectrum covering the whole LWS range, in order to determine possible fringes.

The date were processed using the ISO spectral analysis package (ISAP).

Send offprint requests to: W.H. Kegel (Kegel@astro.uni-frankfurt.de)

* Based on observations made with ISO, an ESA project with instruments funded by ESA Member States (especially the PI countries: France, Germany, the Netherlands and the United Kingdom) and with participation of ISAS and NASA.

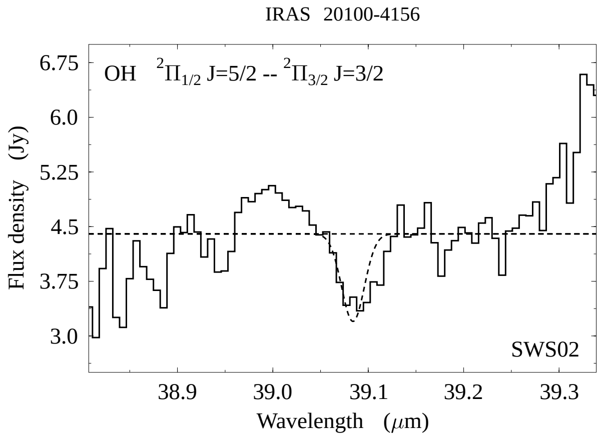

Fig. 1. The spectrum of IRAS 20100-4156 around the (redshifted) position of the 34 μ line of OH. Superposed on the observational data (solid line) is a calculated line width of the instrumental profile (dashed line) at the expected position of the OH line.

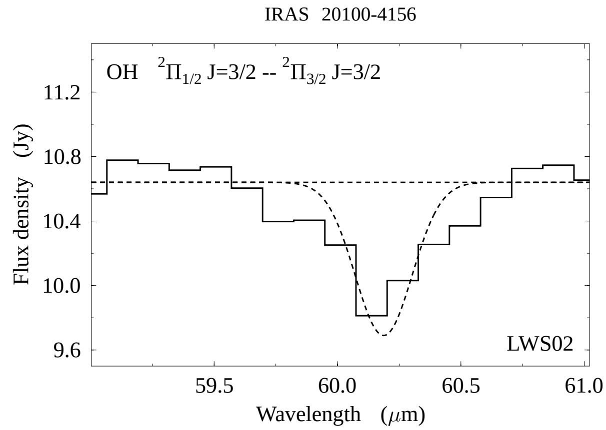

Fig. 2. Same as Fig. 1, but for the 53 μ line of OH.

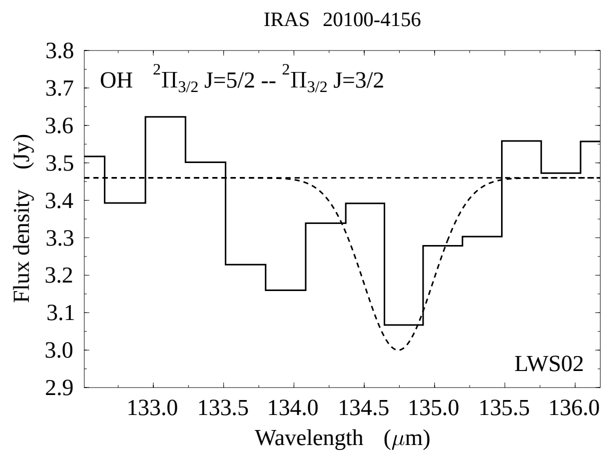

Fig. 3. Same as Fig. 1, but for the 119 μ line of OH.

Table 1. Observational parameters

Date	AOT	Observing time [s]
	IRAS 20100-4156	
18 Oct. 96	SWS02	6950
9 Nov. 96	LWS02	12568
23 Mar. 98	LWS02	5762
	3 Zw 35	
16 Jul. 97	SWS02	2460
10 Aug. 97	LWS01	1604
10 Aug. 97	LWS02	6442

Table 2. W_λ/λ

Line	IRAS 20140	3Zw35
34 μ	$(2.6 \pm 0.4) \cdot 10^{-4}$	$(2.1 \pm 0.5) \cdot 10^{-4}$
53 μ	$(6.0 \pm 0.9) \cdot 10^{-4}$	$(4.5 \pm 1.6) \cdot 10^{-4}$
119 μ	$(5.0 \pm 2.2) \cdot 10^{-4}$	$< 5 \cdot 10^{-4}$

3. Results

Our targets are so faint that we had to use quite long integration times. Nevertheless, the spectra are rather noisy. Therefore our measurements are not very accurate. One major problem was to define the continuum, which showed in some cases an unrealistic apparent wavelength dependence (see in particular Fig. 1 and Fig. 4). We did not subtract the off-source from the on-source spectra since the off-source spectra do not correspond to white noise but show spurious structures. This introduces an additional uncertainty in the measurement of the continuum. In particular the equivalent width of the 53 μ line may be affected by this.

It appears that our measurements were at the limit of what could be achieved with the ISO spectrometers. To our knowledge this is the first detection of OH lines in LWS spectra of OH megamaser galaxies.

3.1. IRAS 20100-4156

The lines at 34 μ and 53 μ are clearly detected in absorption (Figs. 1 and 2). There appears to be some absorption at the position of the 119 μ line (Fig. 3), but it is definitly much weaker than one would expect according to the strengths of the lines at 34 μ and 53 μ. From the latter one may derive an estimate for the OH column density. The spectral resolution (1400 and 200, respectively) is not sufficient to resolve the line profiles. (In the case of the 34 μ line, however, one can see that the line is wider than the instrumental profile, as expexted from the $\Lambda-$ splitting.) The quantity to be measured is the equivalent width

$$W_\lambda = \int \frac{I_{\rm cont} - I_\lambda}{I_{\rm cont}} d\lambda \quad . \tag{1}$$

For the redshift independent quantity W_λ/λ we measured the values given in Table 2.

In order to estimate the column density we consider the simple model of a cool OH cloud in front of a bright IR continuum source. For an isolated absorption line then the following relation holds:

$$\frac{W_\lambda}{\lambda} \leq \frac{1}{\lambda} \int \left(1 - {\rm e}^{-\tau_\nu}\right) d\lambda \quad . \tag{2}$$

The equal sign applies in the case that the absorbing cloud fully covers the continuum source and in addition we neglect the spontaneous emission. We further have the relation

$$\frac{1}{\lambda}\int\left(1-\mathrm{e}^{-\tau_\nu}\right)d\lambda \leq \frac{1}{\nu}\int \tau_\nu d\nu \tag{3}$$

and thus

$$\frac{W_\lambda}{\lambda} \leq \frac{h}{c}\left(N_{\mathrm{l}}-\frac{g_{\mathrm{l}}}{g_{\mathrm{u}}}N_{\mathrm{u}}\right)B_{\mathrm{abs}} \leq \frac{h}{c}B_{\mathrm{abs}}N_{\mathrm{l}} \tag{4}$$

where N_{l} is the column density of the molecules in the lower level and N_{u} of those in the upper level. B_{abs} is the Einstein coefficient for absorption. Eq. (4) gives a (possibly rather crude) estimate of the coulumn density of the molecules in the lower level, which in our case is the rotational ground state. This estimate is close to the true value only if the line is optically thin and if $N_{\mathrm{u}} \ll N_{\mathrm{l}}$. If one wants to account for optical thickness effects one has to measure at least two lines and to calculate curves of growth. For this one has to know the broadening mechanism. In our particular case it is important to note that we measure the absorption by unresolved multiplets rather than by single lines. In calculating a curve of growth one therefore has to account for the individual components caused by $\Lambda-$doubling and hyperfine splitting.

We calculated curves of growth assuming that the individual components of the multiplets are broadened by a turbulent velocity field. We accounted for this in the microturbulent approximation. Furthermore we considered only the case of pure absorption $\left(N_{\mathrm{u}} \ll N_{\mathrm{l}}\right)$, which is a reasonable assumption as long as the excitation temperature is well below the excitation energy of the upper level. Finally we assumed that the relative population of the individual levels of the rotational ground state corresponds to their statistical weight. This means, we calculated W_λ from (2) with

$$\tau_\nu = N_{OH}\frac{h\nu_0}{c}\sum_{i=1}^{L}\frac{B_{abs}^{(i)}g_i}{\sum_j g_j}\Phi_i(\Delta\nu)\,, \tag{5}$$

$$\Phi_i(\Delta\nu) = \frac{1}{\Delta\nu_D\sqrt{\pi}}\,exp\{-\left(\frac{\Delta\nu}{\Delta\nu_D}\right)^2\}\,, \tag{6}$$

and

$$\Delta\nu = \nu-\nu_i = \nu-\nu_0+(\nu_0-\nu_i) \tag{7}$$

L is the number of components of a given multiplet (6 for the $34\,\mu$ line and 8 for the $53\,\mu$ line). The index i refers to the individual components. The ν_i designate the central frequencies while ν_0 is an arbitrary reference frequency. The Doppler width is given by

$$\left(\frac{\Delta\nu_D}{\nu_0}\right)^2 = \frac{1}{c^2}\left(v_{th}^2+\sigma^2\right) \approx \frac{\sigma^2}{c^2}\,, \tag{8}$$

where v_{th} and $(\sigma/\sqrt{2})$ are the thermal and the turbulent velocities, respectively. The thermal velocity is negligible as compared to the turbulent velocity derived from the measured data. Since the number of components and the splitting is different for the two lines, we calculated separate curves of growth for the $34\,\mu$ and the $53\,\mu$ line, respectively, and determined the parameter pair σ and N_l for which the computed values of W_λ of both lines coincide with the measured ones. In Table 3 we collect the most essential line data. The first column gives the (rest frame) wavelength, the second gives the corresponding excitation energy in units of K, the third one gives the Einstein $B-$value for absorption of the strongest hyperfine component, and the last column gives the $\Lambda-$doubling in units of $\mathrm{km\,s^{-1}}$.

Table 3. Line data

Line	$\frac{hc}{k\lambda}$ [K]	B_{abs} $\left[\mathrm{cm^3/erg\ sec^2}\right]$	$\Lambda-$splitting $\left[\mathrm{km\,s^{-1}}\right]$
$34\,\mu$	423	$6.6\cdot10^{15}$	224
$53\,\mu$	272	$3.7\cdot10^{16}$	509
$119\,\mu$	121	$2.1\cdot10^{18}$	527
$115\,\mu$	125	$2.0\cdot10^{16}$	614
18 cm	0.08	$2.7\cdot10^{18}$	

From the equivalent widths of the $34\,\mu$ and the $53\,\mu$ line, respectively, we derive by this curve of growth analysis for the column density the estimate

$$N_{OH} \approx (2.2\pm0.4)\cdot10^{17}\mathrm{cm}^{-2}. \tag{9}$$

The microturbulent velocity (b-parameter) is estimated to be $(100\pm25)\,\mathrm{km\,s^{-1}}$. We note that this is the parameter used to calculate the curves of growth. The actual turbulent velocity may be larger if spatial correlations are important since in this case the curve of growth for a given value of σ starts to flatten at a lower column density (Levshakov & Kegel 1996).In addition an analysis based on a mesoturbulent model also may lead to a higher value of the column density. However, in view of the limited quality of our data we do not consider it appropriate to go into a more detailed analysis (which also would introduce one more free parameter). - The value (9) for the column density is in good agreement with the value one derives from $W_\lambda\,(34\,\mu)$ using the crude estimate (4). This, as well as the curve of growth analysis, indicates that the $34\,\mu$ line is still close to the linear part of the curve of growth. This latter fact implies in retrospect that the value derived for the column density is quite independent of the details of the analysis.

It is obvious that the tentatively measured equivalent width of the $119\,\mu$ line is inconsistent with that of the other lines. Since the Einstein $B-$value for absorption of the $119\,\mu$ line is a factor of 57 larger than that of the $53\,\mu$ line, the equivalent width also should be larger. According to the model parameters determined from the $34\,\mu$ and the $53\,\mu$ line, the equivalent width of the $119\,\mu$ line should be a factor of 3 larger than the measured value. According to our observations (Fig. 3) so large a value can be ruled out. - One way to interpret the weakness of the $119\,\mu$ line would be to assume that the continuum source is more extended at $119\,\mu$ than at $34\,\mu$ and $53\,\mu$ and that at $119\,\mu$ the absorbing cloud does not fully cover the continuum source.(A covering factor of 0.3 would be consistent with the observation.)

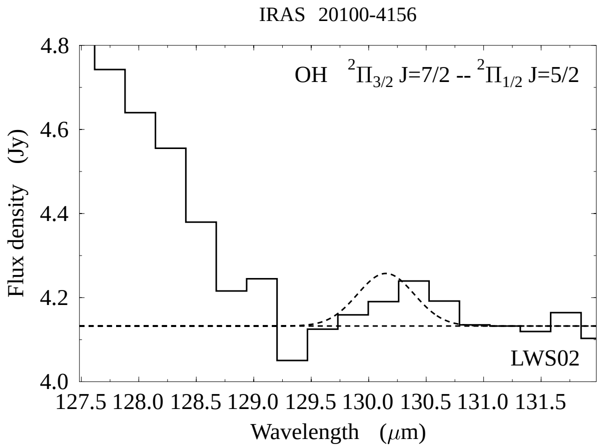

Fig. 4. Same as Fig. 1, but for the 115 μ line of OH.

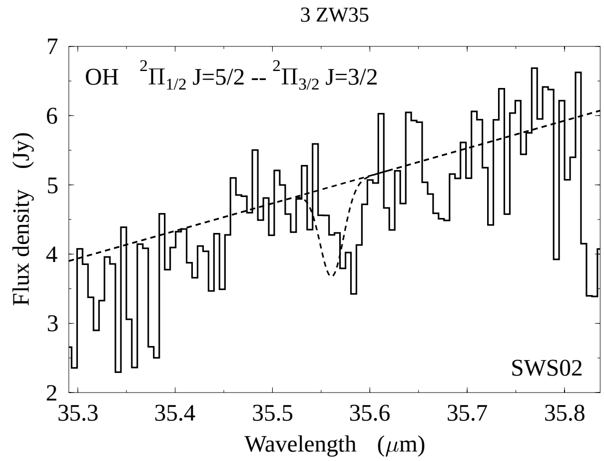

Fig. 5. Spectrum of 3Zw35 around the (redshifted) position of the 34 μ line of OH. Superposed on the observational data (solid line) is a calculated line width of the instrumental profile (dashed line) at the expected position of the OH line.

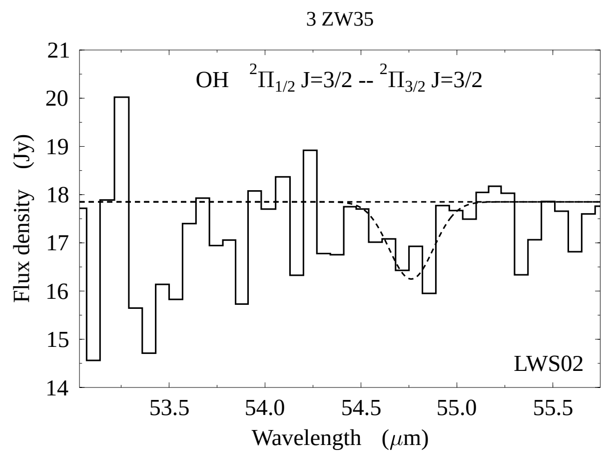

Fig. 6. Same as Fig. 5, but for the 53 μ line of OH.

This assumption appears to be plausible if one considers the IR continuum to be emitted by dust heated by a central source. In this case the warmer dust, emitting at 34 μ and 53 μ, would be more locally concentrated than the cooler dust emitting at 119 μ. - Another explanation for the low absorption observed for the 119 μ line may be the possibility that the absorption in the light of the bright central source is partially compensated by line emission from other parts in the galaxy. The upper level of the 119 μ line may be excited by collisions in warmer regions (see Table 3) leading to an emission line if there is no bright IR background. The spatial resolution of ISO ($\approx$ 200 kpc for $z = 0.129$) is low compared to the size of the galaxy.

As mentioned in the introduction, the primary aim of this project was to search for an emission in the 115 μ line. Such an emission could not be found with any certainty (see Fig. 4). At the (redshifted) position of the 115 μ line there is with certainty no absorption. The apparent very weak $\left(W_\lambda/\lambda \approx 1.2 \cdot 10^{-4}\right)$ emission is not reliable. One problem is the steep rise of the apparent continuum towards shorter wavelengths, which probably is caused by an instrumental effect since we see a similar rise in the off-source spectrum. - In view of the poor quality of the data the non-detection of the 115 μ line does not allow any firm conclusion. Moreover, the argument given with respect to the 119 μ line, that the continuum source may be sustantially more extended than at 34 μ and 53 μ, applies to the 115 μ line as well.

3.2. 3 Zw 35

The spectra we obtained for 3 Zw 35 are considerably more noisy than those for IRAS 20100-4156. There seems to be some absorption at the positions of the 34 μ (Fig. 5) and the 53 μ line (Fig. 6). In the vicinity of the position of the 53 μ line there are other line-like structures which may be fringes. However a more detailed analysis could not identify a strict periodicity. The wavelength interval covered by our measurement is so short that this problem could not be resolved. (The quality of the LWS01 spectrum was also not sufficient.) If we take the measured equivalent widths of the 34 μ and the 53 μ line, respectively, at face value, we derive for the column density

$$N_{OH} \approx (2.0 \pm 0.6) \cdot 10^{17} \text{cm}^{-2} \tag{10}$$

and for the microturbulent velocity a value of (80 ± 20) km s^{-1}. The spectra at the positions of the 119 μ and the 115 μ line are extremely noisy and no indication for a spectral line, neither in absorption nor in emission, could be detected $\left(W_\lambda/\lambda < 5 \cdot 10^{-4}\right)$.

4. Discussion

We estimated for two OH megamaser galaxies the OH column densities. Despite the fact that these two galaxies differ in their 1667 MHz luminosity by about a factor of 20 and in their IR luminosity by about a factor of 7, the derived values for N_{OH} are about the same. This finding supports the hypothesis that OH megamasers are radiatively pumped, since the column density (more precisely the column density over the line width) is the most important parameter determining radiative transfer effects. If the maser is pumped by just one IR line, one would expect the maximal output in the maser line at a given intensity of the pump radiation when the optical depth in the pump line is about unity.

If the optical depth is small compared to unity, most of the pump photons pass through the OH cloud without being absorbed. If, on the other hand, the optical depth is very large, the larger part of the cloud is not pumped at all. In the unpumped region the absorption coefficient for the 1667 MHz line is positive, implying that the maser radiation emitted at the backside of the cloud is reabsorbed when passing through the unpumped region. - In this context we note that, assuming a microturbulent velocity of $100\,\mathrm{km\,s^{-1}}$, the central optical depth of the lines at 34 μ, 53 μ, 79 μ and 119 μ becomes unity (accounting for $\Lambda-$splitting, but not for hyperfine splitting) for $N_{OH}[\mathrm{cm}^{-2}] = 4.6 \cdot 10^{17}$, $7.4 \cdot 10^{16}$, $3.7 \cdot 10^{16}$ and $1.4 \cdot 10^{15}$, respectively. Thus, the column densities derived for IRAS 20100-4156 and 3Zw35 are consistent with the general view that OH megamasers are pumped by the 34 μ and/or the 53 μ lines.

This is a very general argument not refering to any detail of the pumping mechanism. In this context we further note that Skinner et al. 1997 observed the 34 μ line in the spectrum of Arp 220, another OH megamaser galaxy. From their spectrum we determined $W_\lambda/\lambda = 2.76 \cdot 10^{-4}$, implying a lower limit for the column density of $N_{OH} \geq 1.9 \cdot 10^{17}\mathrm{cm}^{-2}$. By a somewhat more detailed analysis the authors derive $N_{OH} = 4 \cdot 10^{17}\mathrm{cm}^{-2}$.

Acknowledgements. This work was stimulated by an intense discussion of W. H. K. with R. Genzel. We further acknowledge support from the ISO Spectrometer Data Centre at MPE Garching, funded by DARA under grant 50 QI 9402 3, and thank in particular D. Kunze and E. Sturm for their help. The data reduction was performed using the ISO Spectral Analysis Package (ISAP), which is a joint development by the LWS and SWS Instrument Teams and Data Centers. Contributing institutes are CESR, IAS, IPAC, MPE, RAL, and SRON. We acknowledge constructive criticism by the referee Dr. V. Bujarrabal. This work was supported by the Deutsche Zentrum für Luft- und Raumfahrt (DLR) under grant 50 OR 95020.

References

Chapman J.M., Staveley-Smith L., Axon D.J., et al., 1990, MNRAS 244, 281
Duc P.-A., Mirabel I.F., Maza J., 1997, A&AS 124, 533
Levshakov S.A., Kegel W.H., 1996, MNRAS 278, 497
Skinner C.J., Smith H.A., Sturm E., et al., 1997, Nat 386, 472
Staveley-Smith L., Allen D.A., Chapman J.M., Norris R.P., Whiteoak J.B., 1989, Nat 337, 625